# Relaxation oscillations induced by amplitude-dependent frequency in dissipative trapped electron mode turbulence

P. W. Terry, A. S. Ware, and D. E. Newman[a)]
*Department of Physics, University of Wisconsin—Madison, Madison, Wisconsin 53706*

(Received 3 June 1994; accepted 9 September 1994)

A nonlinear frequency shift in dissipative trapped electron mode turbulence is shown to give rise to a relaxation oscillation in the saturated power density spectrum. A simple non-Markovian closure for the coupled evolution of ion momentum and electron density response is developed to describe the oscillations. From solutions of a nonlinear oscillator model based on the closure, it is found that the oscillation is driven by the growth rate, as modified by the amplitude-dependent frequency shift, with inertia provided by the memory of the growth rate of prior amplitudes. This memory arises from time-history integrals common to statistical closures. The memory associated with a finite time of energy transfer between coupled spectrum components does not sustain the oscillation in the simple model. Solutions of the model agree qualitatively with the time-dependent numerical solutions of the original dissipative trapped electron model, yielding oscillations with the proper phase relationship between the fluctuation energy and the frequency shift, the proper evolution of the wave number spectrum shape and particle flux, and a realistic period. © *1994 American Institute of Physics.*

## I. INTRODUCTION

The microscale fluctuations of tokamak plasmas are generally regarded as stationary and treated as being driven by gradients that are time independent (i.e., fixed or maintained). Turbulence driven by fixed gradients is typically presumed to have a growth rate that does not vary as the amplitudes evolve from the linear phase into the nonlinear phase and saturation. This presumption is implicit in the mixing length, but, in fact, underlies more sophisticated treatments that explicitly calculate renormalized diffusivities.[1] The notion of a fixed growth rate allows the fluctuation level to be obtained as the solution of an effectively linear equation for the RMS amplitude at which the fixed rate of energy input (growth rate[2]) balances the amplitude-dependent rate of nonlinear spectral transfer. This balance is simplified by the fact that for a stationary state, the time-history integrals of statistical closure theories can be Markovianized, yielding transfer rates that are instantaneous functions of the amplitude. Variations on this stationary balance are able to account for incoherent fluctuations and incoherent emission, but still treat the growth rate of normal modes as amplitude independent.[3,4] In recent years, a number of turbulence models have been examined in which the growth rate is modified at finite amplitude and in saturation, even when gradients remain fixed.[5–7] Saturation in these cases involves changes in the fluctuation structure that alter the rate of free energy extraction, but is still presumed to be stationary.

In this paper we present an examination of plasma turbulence that violates both the notion of a fixed growth rate (even in local theory, where the spatial eigenmode structure is not treated) and the assumption of stationarity of saturation. The breakdown of these notions is rooted in universal but generally overlooked aspects of propagating plasma instabilities: the fact that the growth rate $\gamma$ depends on the oscillation frequency $\omega_r$, and that $\omega_r$ tends to be modified at finite amplitude. The former is a well-known feature of drift waves, the growth rate being proportional to the difference of the diamagnetic frequency and the fluctuation frequency. Because the diamagnetic frequency typically exceeds the fluctuation frequency, increases in the fluctuation frequency lead to decreases in the growth rate. Changes in the fluctuation frequency at finite amplitude are also a feature of drift wave and trapped particle mode turbulence.[8–12] The shifting of the fluctuation frequency at finite amplitude possibly arises from more than one nonlinear mechanism, and can be of sufficient magnitude to significantly modify the growth rate, saturation balance, and fluctuation level. Changes in the growth rate (or free-energy extraction rate) due to frequency shifts should thus be regarded as a potentially important aspect of saturation, just as changes in the growth rate due to nonlinear modification of the fluctuation structure have been shown to alter saturation in nonlocal theory.[5–7]

In this work, the role of nonlinear frequency shifts in the saturation of dissipative trapped electron mode turbulence is examined. From previous work, unstable dissipative trapped electron modes are known to experience a marked upshift in RMS frequency at finite amplitude, provided their wave numbers are in the spectral region, where both the $E\times B$ and polarization drift nonlinearities are operative.[10,11] This shift is associated with triads that couple through both nonlinearities via the standard statistical couplings that survive phase scrambling, and hence lead to closure. Numerical simulation of dissipative trapped electron mode turbulence has shown that the cross-coupling frequency shift leads to a saturated state that is *intrinsically nonstationary*.[13,14] Specifically, the saturated state is characterized by large-amplitude, long period relaxation oscillations in the total fluctuation energy, power density spectrum, and particle flux. Such oscillations cannot be described by steady-state balances and violate the Markovian reduction that applies to *the steady* state.

[a)]Present address: Oak Ridge National Laboratory, Oak Ridge, Tennessee 37831.

 1070-664X/94/1(12)/3974/12/$6.00 

In the present work we explore the plausibility of a hypothesis[13] for the basic relaxation oscillation as a cycle in which (1) frequency shifts are generated in unstable modes as the RMS amplitude nears the saturation level; (2) the reduction in growth rate caused by the frequency shifts puts the modes in an over-saturated state, and their amplitude falls to a lower level compatible with the reduced growth; and (3) at the lower level the frequency shifts are now smaller and the growth rate increases. This puts the modes in an under-saturated condition and their amplitude must increase, restarting the cycle. A key issue is identification of the physical mechanism providing the effective inertia necessary to prevent the restoring force from simply forcing the saturation to a lower stationary level.

In order to test the validity of the above hypothesis, a model for dissipative trapped electron mode turbulence is adopted that allows for analytic treatment that properly describes the feedback of frequency shifts on the growth rate and on the dynamics of saturation. This model combines the equations for electron density response and the ion momentum to form an equation that is nominally second order in time. However, as noted in Ref. 15, a two time scale treatment of the equation must be used in order for the electron density to remain a response to the potential. In Ref. 15, the model was solved numerically in the context of coherent structure dynamics; here, an analytic treatment is developed to describe the relaxation oscillation phenomenon. The two time scale procedure places particular constraints on the closure and its solution and ultimately yields coupled equations for the spectrum evolution and the amplitude-dependent growth rate, as detailed in Secs. III and IV.

The salient elements of this study are now summarized.

(i) The model and solution procedure yield a relatively simple description of the nonlinear dynamics of the cross-correlation of density and potential (particle flux), a long-standing problem in drift wave physics. The cross-correlation dynamics are lost in so-called "$i\delta$" approximations,[8–9,11] and are governed by complicated expressions in renormalized theories of the cross-correlation.[16–17] Here they emerge from the solution of the equation that governs the temporal evolution of the amplitude-dependent growth rate normalized to the shifted frequency. Because the growth rate is governed by amplitudes at prior times, the oscillation of the particle flux lags behind the amplitude oscillation by a correlation time.

(ii) The frequency shift induced by the cross-coupling of the $E\times B$ and polarization drift nonlinearities itself depends on the frequency, a fact overlooked in previous analyses.[10,11] From the renormalization, this dependence is found to reduce the frequency shift, causing it to saturate as the fluctuation level increases. The maximum possible frequency shift occurs as the amplitude tends to infinity and makes unstable modes become marginally stable. Thus, it is not possible to make a growing mode become damped, and *vice versa*. These results are consistent with the fact that a marked increase in the frequency shift is observed in simulations when the frequency dependence is excluded.

(iii) A set of saturation relations is derived that describes nonstationary saturation and is amenable to approximate solutions and modeling. This set of equations is derived from the Direct Interaction Approximation (DIA),[18] which in its standard form is poorly suited for simple representation of the present problem, because it is analytically intractable and yields the growth rate only upon solution of the nonlinear response function equation. Because the period of the relaxation oscillation is only somewhat longer than the correlation time, the time history effects of the closure must be retained. These arise because each member of an interacting triad is governed by the time integrated effect of its interaction with other modes during the previous correlation time. The two time scale solution of the response function equation and an expansion of the time history integral yield an evolution equation for the growth rate that is driven by the difference of the actual growth rate and the instantaneous or Markovian growth rate.

(iv) The nonstationary saturation relations are readily reduced to a nonlinear oscillator or extended predator–prey model. This is accomplished by partitioning the spectrum into discrete ranges and evolving the energy in each range. This system is to the nonstationary saturation relations what the mixing length is to stationary saturation. The system reduces to the mixing length identity under the assumption of stationarity, satisfies the energy conservation constraints of the original closure equations, and incorporates the effects of time history in the growth rate evolution.

(v) With the extended predator–prey system, it is possible to explore the question of what physical process produces the effective inertia required to maintain the relaxation oscillation. Two mechanisms are examined. One is the inertia associated with the finite time of transfer of energy among spectrum components. This mechanism is manifested in the coupling of components, with each driven by a first-order equation. This coupling constitutes a form of memory, inasmuch as formal inversion of one evolution equation and substitution in the others produces time-history integrals in the coupling coefficients.[19] The second mechanism is that of the memory associated with the statistical closure and manifests itself as the drive of the growth rate evolution. Removing the latter produces stable fixed point solutions in systems with two or three spectrum components. Including it yields limit cycle solutions. This indicates that the memory of the growth rate of prior amplitudes, through the time-history integrals of the closure, is the effective inertia, not the finite time of transfer in the spectrum.

From numerical solutions of the oscillator model, the basic qualitative properties of the relaxation oscillation observed in numerical solutions of the primitive equations are recovered. These include the correct temporal correlation or phase between the oscillations of the fluctuation energy and the frequency shift, the correct evolution of the wave number spectrum shape, as manifested in the phase of oscillations of the amplitude of various wave number bands, and realistic oscillation periods. The amplitude tends to be slightly larger than values observed in simulation of the basic equations, and may be due to the fact that the entire spectrum is being represented by only two or three modes in the oscillator model. The oscillator model shows that the relaxation oscillations make a transition to a fixed point (stationary solution)

when the response of the frequency shift to a change in amplitude is more rapid than a nonlinear correlation time. This demonstrates the fact that non-Markovian elements of the turbulent interaction are essential to the relaxation oscillation phenomenon and provides a clear example of a failure of Markovian assumptions.

This paper is organized as follows: in Sec. II the model equations are presented and their properties are discussed. To simplify analysis and avoid the difficulties posed by cross-correlations, a second-order (in time) one-field model is used instead of a two-field model. In Sec. III we present the derivation of the renormalized equations, frequency shift, and frequency shift modified growth rate. An expansion of the time history integrals arising from the closure is introduced in Sec. IV. In Sec. V we detail several nonlinear oscillator models derived from the saturation equations and present numerical solutions. Section VI gives the conclusions.

## II. MODEL AND PROPERTIES

Trapped electron modes can be described by fluid equations governing the evolution of the trapped electron density and a neutralizing ion density. Quasineutrality with the full electron density, including adiabatic electrons, provides a closed system:

$$\frac{\partial n_e}{\partial t}-C_s\rho_s\,\nabla\phi\times\mathbf{z}\cdot\nabla n_e+\nu_{\rm eff}n_e=-\frac{\partial\phi}{\partial t}-V_D(1+\alpha\eta_e)\,\frac{\partial\phi}{\partial y}, \tag{1}$$

$$\frac{\partial n_i}{\partial t}-C_s\rho_s\,\nabla\phi\times\mathbf{z}\cdot\nabla n_i-\rho_s^2\nabla^2\,\frac{\partial\phi}{\partial t}$$

$$+\rho_sC_s\,\nabla\phi\times\mathbf{z}\cdot\nabla\rho_s^2\,\nabla^2\phi=-V_D\,\frac{\partial\phi}{\partial y}, \tag{2}$$

and

$$\epsilon^{1/2}n_e+\phi=n_i, \tag{3}$$

where $n_e$ and $n_i$ are the trapped electron and ion densities, normalized to the mean density, $\phi$ is the potential, normalized to $T_e/e$, $V_D=(cT_e/eB)L_n^{-1}$ is the diamagnetic drift velocity, $C_s=(T_e/m_i)^{1/2}$ is the ion sound speed, $\rho_s=(cT_e/eB)/C_s$ is the ion gyroradius evaluated at the electron temperature, $\eta_e=d\ln T_e/d\ln n_e$ is the ratio of the electron density and temperature gradient scale lengths, $\nu_{\rm eff}=\nu_e/\epsilon$, $\alpha=\frac{3}{2}$ represents the magnitude of the thermal component of equilibrium gradients in the diamagnetic drift, and $\epsilon^{1/2}=(r/R)^{1/2}$ is the trapped electron fraction.

These equations provide a minimal model of the physics of trapped electron mode turbulence. Their basic properties have been discussed in Refs. 13 and 20, and will not be repeated here. For the dissipative trapped electron regime, the nonadiabatic electron density is effectively laminar, i.e., the electron inertia $dn_e/dt$, which includes the electron nonlinearity, is small compared to the collisional dissipation $\nu_{\rm eff}n_e$. The nonadiabatic electron density is therefore given by

$$n_e=-\frac{1}{\nu_{\rm eff}}\left(\frac{\partial\phi}{\partial t}+(1+\alpha\eta_e)V_D\,\frac{\partial\phi}{\partial y}\right), \tag{4}$$

and the growth rate, which goes as the Fourier transform of this expression, is proportional to $\omega-\omega_*(1+\alpha\eta_e)$, where $\omega_*=V_Dk_y$. The dependence on $\omega$ comes from the inertia of adiabatic electrons and provides the link between frequency and growth rate. Since the linear frequency is close to $\omega_*$ there is partial cancellation between $\omega$ and $\omega_*(1+\alpha\eta_e)$, and nonlinear frequency shifts of order $\omega_*$ can have a significant effect on the growth rate.

A one-field equation for the dissipative regime is obtained by using Eq. (3) to eliminate $n_i$ in Eq. (2), and substituting for $n_e$ from Eq. (4) to yield

$$\frac{\partial\phi}{\partial t}-\rho_s^2\nabla^2\,\frac{\partial\phi}{\partial t}-\frac{\sqrt{\epsilon}}{\nu_{\rm eff}}(1+\alpha\eta_e)V_D\,\frac{\partial}{\partial t}\,\frac{\partial\phi}{\partial y}-\frac{\sqrt{\epsilon}}{\nu_{\rm eff}}\,\frac{\partial^2\phi}{\partial t^2}$$

$$+C_s\rho_s^3\,\nabla\phi\times\mathbf{z}\cdot\nabla\nabla^2\phi-\frac{\sqrt{\epsilon}}{\nu_{\rm eff}}\,C_s\rho_s\nabla$$

$$\times\left(\frac{\partial\phi}{\partial t}+(1+\alpha\eta_e)V_D\,\frac{\partial\phi}{\partial y}\right)\times\mathbf{z}\cdot\nabla\phi=-V_D\,\frac{\partial\phi}{\partial y}. \tag{5}$$

As noted in Ref. 15, equations of this type are nominally second order in time, but must be solved perturbatively with terms proportional to $\omega/\nu_{\rm eff}$ treated in higher order. Since the highest time derivative is $O(\omega/\nu_{\rm eff})$, the lowest-order solution is effectively first order in time. This properly maintains the electron equation as a response to the potential and identifies the physical root of the dispersion relation as the nonsingular root (in the limit $\omega/\nu_{\rm eff}\to 0$). Solving the dispersion relation for this root yields

$$\omega^{(0)}=\frac{\omega_*}{(1+k^2\rho_s^2)}, \tag{6}$$

$$\omega^{(1)}=-i\gamma$$

$$=i\,\frac{\sqrt{\epsilon}}{\nu_{\rm eff}}\,\omega^{(0)}[\omega^{(0)}-(1+\alpha\eta_e)\omega_*]$$

$$=-i\,\frac{\sqrt{\epsilon}}{\nu_{\rm eff}}\,\frac{\omega_*^2}{(1+k^2\rho_s^2)^2}\,[\alpha\eta_e+k^2\rho_s^2(1+\alpha\eta_e)]. \tag{7}$$

The lowest-order dispersion yields the real frequency, Eq. (6), and the next order yields the growth rate, Eq. (7). As indicated, the growth rate is proportional to $\omega-\omega_*(1+\alpha\eta_e)$. In linear theory, $\omega$ is given by Eq. (6), yielding Eq. (7); at or near saturation, Eq. (6) will be modified by the addition of an amplitude-dependent frequency, leading to changes in the growth rate.

The presence of the $E\times B$ nonlinearity [the last term on the left-hand side of Eq. (5)] in a one-field evolution model implies that energy is the only quadratic quantity held invariant by the nonlinear transfer dynamics.[8,11] Although energy is conserved by the nonlinear transfer dynamics, it is by no means a constant in the saturated state. In simpler models that neglect the adiabatic electron inertia,[8,11] energy is a constant, because the linear growth rate is fixed and the transfer rate is a conservative, monotonic function of amplitude. By contrast, in the present model, the saturation energy need not be a constant. This is because frequency shifts can modify the growth rate or rate of energy injection into the modes.

## III. RENORMALIZED SATURATION BALANCE

The saturated state of dissipative trapped electron mode turbulence can be accurately described using the standard statistical ansatz of closure theory,[21] i.e., the assumption that the fourth-order cumulant is negligible. However, a number of additional simplifying assumptions are often introduced into closure equations. These assumptions reduce complicated closures, such as the DIA,[18] to a form more conducive to analytic solution of the saturation balance and spectrum balance equations. The two primary assumptions are the Markovian approximation of the time history integrals that appear in renormalized diffusivities, and representation of the nonlinear response function of the turbulent medium as an exponential decay with a self-similar eddy diffusivity. These are the basis of the widely used Eddy Damped QuasiNormal Markovian (EDQNM) closure.[21]

It is not possible to describe the relaxation oscillation phenomenon with EDQNM closures. The equation for the nonlinear response function must be obtained and solved in order to correctly determine the nonlinearly modified growth rate, and time history effects *must be retained* in the expression for the growth rate. In this and the following section, a procedure is introduced that effectively allows an eddy damping representation, but retains the time history effects. This procedure yields an evolution equation for the nonlinearly modified growth rate; which is combined with the spectrum evolution equation (driven by the nonlinearly modified growth rate) to describe saturation. These equations readily lend themselves to the construction of the extended predator–prey system used in Sec. V to model saturation.

The standard iterative closure procedure is applied to the Fourier transformation of Eq. (5) and the energy evolution equation [constructed by multiplying the Fourier transformation of Eq. (5) by $\phi_k^*$ and taking the real part], to yield

$$L_{\mathbf{k}}\phi_{\mathbf{k}}=\left[ i\omega(1+\xi_k+k^2\rho_s^2)+\frac{\sqrt{\epsilon}}{\nu_e}\,\omega[\omega-(1+\alpha\eta_e)\omega_*] - i\omega_*+\gamma_{nl}(k)-i(1+\alpha\eta_e)\omega_*\xi_k\right]\phi_{\mathbf{k}}=0, \tag{8}$$

for the response function, and

$$\left(-\mathrm{Im}\ \omega(1+k^2\rho_s^2)+\frac{\sqrt{\epsilon}}{\nu_e}\,\mathrm{Re}\ \omega[\mathrm{Re}\ \omega-(1+\alpha\eta_e)\omega_*] - \frac{\sqrt{\epsilon}}{\nu_e}(\mathrm{Im}\ \omega)^2\right)|\phi_{\mathbf{k}}|^2+\{\mathrm{Re}[\gamma_{nl}(\omega,k)] - \mathrm{Re}[i\omega_{nl}(\omega,k)]\}|\phi_{\mathbf{k}}|^2-2\ \mathrm{Re}\ L_{\mathbf{k}}^{-1}\sum_{\mathbf{k}'}(|\chi_{\mathbf{k},\mathbf{k}'}^{E\times B}|^2 + |\chi_{\mathbf{k},\mathbf{k}'}^{\mathrm{pol}}|^2)|\phi_{\mathbf{k}'}|^2|\phi_{\mathbf{k}-\mathbf{k}'}|^2=0, \tag{9}$$

for the spectrum evolution equation. Here, $\gamma_{nl}(k)$ is the coherent eddy damping rate, given by

$$\gamma_{nl}(k)=\sum_{\mathbf{k}'}(\mathbf{k}'\times\mathbf{z}\cdot\mathbf{k})^2L_{\mathbf{k}-\mathbf{k}'}{}^{-1}\,\frac{1}{2}\,C_s^2\rho_s^2\left(k_\perp^2(k_\perp^2-k_\perp'^2)\rho_s^4 + \frac{2\epsilon}{\nu_e^2}[\omega'-(1+\alpha\eta_e)\omega_*']^2\right)|\phi_{\mathbf{k}'}|^2, \tag{10}$$

$\xi_k$ is the amplitude factor associated with the cross-coupling frequency shift,

$$\xi_k=\sum_{\mathbf{k}'}(\mathbf{k}'\times\mathbf{z}\cdot\mathbf{k})^2L_{\mathbf{k}-\mathbf{k}'}{}^{1}\,\frac{1}{2}\,C_s^2\rho_s^4\,\frac{\sqrt{\epsilon}}{\nu_e}(k_\perp'^2-2k_\perp^2)|\phi_{\mathbf{k}'}|^2; \tag{11}$$

$\chi_{\mathbf{k},\mathbf{k}'}^{(E\times B)}$ and $\chi_{\mathbf{k},\mathbf{k}'}^{(\mathrm{pol})}$ are the coupling strengths of the $E\times B$ and polarization drift nonlinearities,

$$\chi_{\mathbf{k},\mathbf{k}'}^{(E\times B)}=i\,\frac{C_s\rho_s\sqrt{\epsilon}}{2\nu_e}(\mathbf{k}'\times\mathbf{z}\cdot\mathbf{k})[\omega'-(1+\alpha\eta_e)\omega_*' - (\omega-\omega')+(1+\alpha\eta_e)\omega_*''], \tag{12}$$

$$\chi_{\mathbf{k},\mathbf{k}'}^{(\mathrm{pol})}=\frac{C_s\rho_s^3}{2}(\mathbf{k}'\times\mathbf{z}\cdot\mathbf{k})[(k_\perp-k_\perp')^2-k_\perp'^2]. \tag{13}$$

In these expressions, the subscript $\mathbf{k}$ represents the four-vector comprised of the three spatial components of the wave number and frequency $\omega$. Likewise, the summations over $k$ include an integral over $\omega$. In Eqs. (10) and (12), $\omega_*'=V_Dk_y'$ and $\omega_*''=V_D(k_y-k_y')$. In writing the coherent eddy damping rate, it has been assumed that the eddy damping for the long-wavelength unstable modes is of primary interest. In this case $\omega\ll\omega'$, yielding a damping rate that is independent of the frequency $\omega$.

The two terms in Eq. (8) proportional to $\xi_k$ constitute the nonlinear frequency shift,

$$\omega_{nl}(\omega,k)\equiv-\omega\xi_k+(1+\alpha\eta_e)\omega_*\xi_k. \tag{14}$$

The form of the frequency shift reflects an assumption that the frequency spectrum is peaked about a frequency that has an odd parity in $k$. Specifically, if $\omega=\omega_*(k)+\omega_{nl}(k)$ with $\omega_{nl}(k)$ an odd parity function, contributions to the frequency shift that are proportional to $\omega'$ and $\omega_*'$ vanish upon summation over $k'$ and integration over $\omega'$. The frequency shift amplitude function, Eq. (11), is a product of the coupling strengths for the $E\times B$ and polarization drift nonlinearities, and thus is weighted to high wave number modes (relative to the unstable modes). The frequency shift differs from previous forms[10,11] because of the $\omega$ dependence, an effect arising from the contribution of adiabatic electron inertia to the $E\times B$ nonlinearity. Without the $\omega$ term, $\omega_{nl}$ is proportional to the amplitude (assuming a strong turbulence regime, where $L\propto\phi$). In this case, the magnitude of the frequency shift is limited only by the fluctuation amplitude. On the other hand, with $\omega$ included, the frequency shift is proportional to $\omega-(1+\alpha\eta_e)\omega_*$, the same factor appearing in the growth rate, Eq. (7). As the nonlinearly shifted frequency approaches the magnitude required to stabilize a mode, the shift therefore weakens and approaches zero. Consequently, $\omega\approx(1+\alpha\eta_e)\omega_*$ or $\omega_{nl}\approx\alpha\eta_e\omega_*$ represents the highest possible frequency that can be achieved, even if the fluctuation level is arbitrarily large. Likewise, the cross-coupling frequency shift cannot stabilize an unstable mode or destabilize a stable mode. Rather, the largest possible frequency shift makes an unstable (or stable) mode marginally stable.

Equations (8) and (9) form a coupled system whose solution yields the nonlinearly modified growth rate and fluctuation spectrum. When Fourier transformed back into the time domain, these quantities fluctuate in time as part of the nonlinear relaxation oscillation phenomenon observed in simulations. As is normally the case, the response function equation, Eq. (8), provides the nonlinear decorrelation time that limits the nonlinear interactions that produce the spectral transfer. Here, it also yields the amplitude-dependent growth rate. The spectrum evolution equation, Eq. (9), describes the evolution of spectral components of energy under the influence of the growth rate, contained in the three parts of the first term, coherent eddy damping, represented by the second term, and incoherent emission, the last term. Equation (9) describes conservative energy transfer in wave number space. Specifically, the incoherent emission cancels the coherent spectral transfer when the equation is summed over $k$. The growth rate terms do not vanish; they represent the nonzero rate of energy input (positive or negative, depending on the wave number). Because this term depends on amplitude through the nonlinear frequency shift, it describes a non-energy-conserving nonlinear process quite distinct from the energy conserving spectral transfer of the second and third terms.

To consistently recover the correct amplitude-dependent growth rate and its effect on the spectrum evolution, these equations must be solved perturbatively for $\omega/\nu_{\rm eff}\ll 1$, as previously noted. This ordering also separates evolution on the rapid time scale of the mode coupling interactions and the longer time scale of the relaxation oscillations. These time scales are denoted by $\omega^{(0)}$ and $\omega^{(1)}$, for the rapid and slow time scales, respectively.

As an energy balance equation, the spectrum evolution equation is phase averaged. Consequently, the lowest-order physically meaningful balance occurs at one order higher than the lowest-order balance of the response function equation. In its lowest order, the spectrum evolution equation can be written as

$$\left((1+k^2\rho_s^2)\frac{\partial}{\partial t}+\frac{\sqrt{\epsilon}}{\nu_e}\,\mathrm{Re}\,\omega^{(0)}[\mathrm{Re}\,\omega^{(0)}-(1+\alpha\eta_e)\omega_*]\right.$$
$$\left.-\frac{\sqrt{\epsilon}}{\nu_e}(\mathrm{Im}\,\omega^{(0)})^2\right)|\phi_{\mathbf{k}}|^2+\gamma_{nl}(\omega^{(0)},k)|\phi_{\mathbf{k}}|^2$$
$$-2\,\mathrm{Re}\,L_{\mathbf{k}}^{-1}\sum_{\mathbf{k}'}(|\chi_{\mathbf{k},\mathbf{k}'}^{(E\times B)}|^2+|\chi_{\mathbf{k},\mathbf{k}'}^{(\mathrm{pol})}|^2)|\phi_{\mathbf{k}'}|^2|\phi_{\mathbf{k}-\mathbf{k}'}|^2$$
$$=0, \tag{15}$$

where $\omega^{(1)}$ has been transformed to the time domain, and the frequency dependence of $L$ and $\chi$ is evaluated at $\omega=\omega^{(0)}$. Here $\partial/\partial t$ represents the slow time scale variation of the spectrum, as driven by small imbalances in the spectral terms as they evolve on the long time scale. The second and third terms in the square brackets yield the amplitude-dependent growth rate, with $\omega^{(0)}$ supplied from the lowest-order solution of the response function equation. The coherent damping and incoherent emission rates vary on the long time scale through their dependence on amplitude.

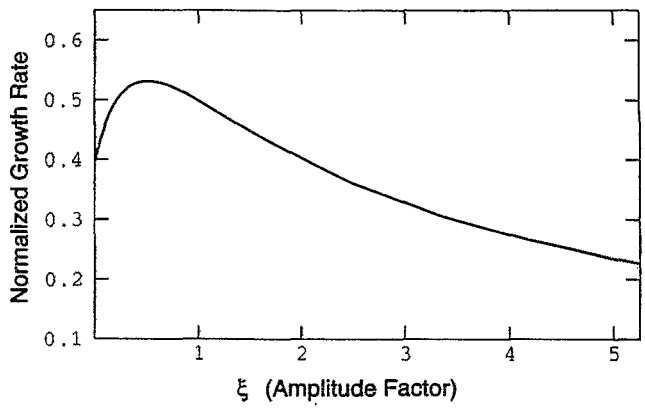


FIG. 1. The growth rate as a function of the amplitude factor $\xi_k$. For $\xi_k=0$, the growth rate reduces to the linear value, while for $\xi_k\to\infty$, the growth rate goes to zero.

To lowest order in $\omega/\nu_e$, the response function yields

$$\omega^{(0)}=\frac{\omega_*+(1+\alpha\eta_e)\omega_*\xi_k}{1+\xi_k+k^2\rho_s^2}, \tag{16}$$

where it is assumed that the saturation amplitude is sufficiently large to make the frequency shift of order $\omega_*$. Both $\gamma_{nl}$ and the growth rate, $(\sqrt{\epsilon}/\nu_e)\omega[\omega-(1+\alpha\eta_e)\omega_*]$ enter in the next order. Note that for $\xi_k$ arbitrarily large (large amplitude), $\omega^{(0)}\sim(1+\alpha\eta_e)\omega_*$. This is precisely the frequency that renders infinitesimal amplitude growing modes marginally stable at large amplitude. Using Eq. (16) to evaluate the growth rate terms in Eq. (15), the spectrum evolution equation becomes

$$\left((1+k^2\rho_s^2)\frac{\partial}{\partial t}+\gamma(t)+\gamma_{nl}\right)|\phi_{\mathbf{k}}|^2-2\,\mathrm{Re}\,L_{\mathbf{k}}^{-1}\sum_{\mathbf{k}'}(|\chi_{\mathbf{k},\mathbf{k}'}^{(E\times B)}|^2$$
$$+|\chi_{\mathbf{k},\mathbf{k}'}^{(\mathrm{pol})}|^2)|\phi_{\mathbf{k}'}|^2|\phi_{\mathbf{k}-\mathbf{k}'}|^2=0, \tag{17}$$

where

$$\gamma(t)=\frac{\sqrt{\epsilon}}{\nu_{\rm eff}}\frac{\omega_*^2}{[1+\xi_k(t)+k^2\rho_s^2]^2}[1+(1+\alpha\eta_e)\xi_k(t)]$$
$$\times[\alpha\eta_e+k^2\rho_s^2(1+\alpha\eta_e)], \tag{18}$$

and $\xi_k(t)$ is given by the temporal Fourier transform of Eq. (11). Equation (18) is the amplitude-dependent growth rate. Comparison with the linear growth rate, Eq. (7), indicates that this expression reduces to the linear growth rate when the fluctuation level goes to zero, and asymptotes to zero when the fluctuation level goes to infinity. The growth rate is plotted in Fig. 1 as a function of $\xi_k$. For saturation levels consistent with mixing length values and $\eta_e$ slightly larger than unity, the growth rate tends to be reduced by as much as 50% at saturation relative to its magnitude at infinitesimal amplitude. In this region, the growth rate decreases strongly with amplitude. For $\eta_e>\frac{2}{3}(=\alpha^{-1})$, the growth rate increases as $\xi_k$ increases from zero, peaking in the range $\frac{1}{2}<\xi_k<1$ (for

$k^2\rho^2=0$), and then decays to zero for higher values. For $\eta_e \leqslant \frac{2}{3}$, the maximum growth rate is at zero amplitude ($\xi_k=0$).

## IV. TIME HISTORY EXPANSION

It is tempting to regard the amplitude-dependent growth rate, coherent damping rate, and incoherent emission rates as being determined by the appropriate spectrum-averaged amplitude at the same instant in time. In fact, all amplitude-dependent rates in turbulence have memory, sensing the prior amplitude history over the time period for which the phases of interacting triplets remain coherent. This memory is a natural consequence of the nonlinear coupling process: time derivatives of wave number spectrum amplitudes are driven by beating with other modes that are evolving under the same coupling process. Because the time derivative is a difference in amplitude over time, amplitudes at prior times directly affect the evolution of wave number spectrum amplitudes.

Time history effects enter in nonlinear rates through the inverse response function $L^{-1}$. In the time domain, this function is replaced by a time integral over all the time-dependent functions to its right, multiplied by the temporal Green's function or propagator associated with the response function. As noted in the previous section, the response function evolves on the faster eddy turnover scale, whereas the spectrum evolves on the slower time scale of the relaxation oscillation. This provides a rationale for the canonical Markovian assumption that is introduced in common eddy damping closures (EDQNM), wherein the spectrum is removed from the time history integral, and the propagator is integrated to obtain a mean correlation time. However, it is essential to retain time history effects if description of the slower time scale evolution of the spectrum is desired, be it the transient approach to a conventional stationary spectrum, or the nonstationary relaxation oscillation of dissipative trapped electron mode saturation.

The object of this section is to represent the memory effects in the growth rate $\gamma(t)$ through its dependence on $\xi_k$, consistent with the two time scale ordering previously introduced. This representation yields the growth rate as the solution of a first-order (in time) differential equation driven by the difference between the actual growth rate and the Markovian growth rate. The derivation of this equation is heuristic, based essentially on dimensional scaling analysis. Therefore it produces only approximate spectrum-averaged rates for each time scale.

In terms of its slower time scale variation, the growth rate of the spectrum evolution equation is given by Eq. (18), where $\xi_k(t)$ is a function of the slowly varying time, obtained from the Fourier transformation of Eq. (11). Thus

$$\xi_k(t)=\sum_{k'} \int^t dt'\ C_{k,k'}G_{k-k'}(t,t')|\phi_{k'}(t')|^2, \tag{19}$$

where

$$C_{k,k'}=(\mathbf{k}\times\mathbf{k}'\cdot\mathbf{z})^2\,\frac{C_s\rho_s^2}{2}\,\frac{\sqrt{\epsilon}}{\nu_{\rm eff}}\,(k'^2-2k^2), \tag{20}$$

$G_{k-k'}(t,t')$ is the propagator of the slow time part of the response function operator,

$$\left(\frac{\partial}{\partial t}\,(1+\xi_k^{(1)})+\gamma(t)+\gamma_{nl}(t)-i(1+\alpha\eta_e)\omega_*\xi_k^{(1)}\right)\times G_k(t,t')=\delta(t-t'), \tag{21}$$

and $\xi_k^{(1)}$ represents the contribution of $\xi_k$ to the slow time scale propagator. The propagator is written as an eddy damping eikonal,

$$G_k(t,t')=\exp[-(t-t')/\tau_k], \tag{22}$$

where $\tau_k$ is the eigenfrequency of the operator of Eq. (21).

Taking the time derivative of $\xi_k(t)$ yields an expression for $\xi_k(t)$ in terms of its Markovian form and corrections of higher order in the two time scale expansion:

$$\begin{aligned}\frac{d}{dt}\,\xi_k(t)&=\sum_{k'}\,C_{k,k'}|\phi_{k'}(t)|^2-\sum_{k'}\,\tau_{k-k'}^{-1}\\&\quad\times\int^t dt'\ C_{k,k'}G_{k-k'}(t,t')|\phi_{k'}(t')|^2\\&\approx C|\phi(t)|^2-\tau^{-1}\xi_k(t),\end{aligned} \tag{23}$$

where the quantities to the right of the last equality are spectrum averaged, and therefore wave number subscripts are dropped. Multiplying this expression by the spectrum averaged decorrelation time $\tau$, the right-hand side is recognized as the difference between the standard Markovian form of $\xi_k(t)$ and $\xi_k(t)$ itself. Thus, $\xi_k(t)$ can be written as its Markovian form, and a non-Markovian correction given in terms of the derivative of $\xi_k(t)$,

$$\xi_k(t)=C|\phi(t)|^2\tau-\tau\,\frac{d}{dt}\,\xi_k(t). \tag{24}$$

As long as the cycle time is long compared to the decorrelation time, $\tau[d\xi_k/dt]/C|\phi(t)|^2\tau=O(\pi/\tau_{\rm cycle})\ll 1$, and this correlation is small.

With Eq. (24), it is now possible to expand the growth rate $\gamma(t)$ about the Markovian $\xi_k$. Substituting Eq. (24) into Eq. (18), and keeping terms up to order $\tau\,d\xi_k/dt$, the growth rate is written as

$$\begin{aligned}\gamma(t)&=\gamma_m(t)\\&\quad+\frac{(\sqrt{\epsilon}/\nu_{\rm eff})\omega_*^2[\alpha\eta_e+(1+\alpha\eta_e)k^2\rho_s^2]\tau(d\xi_k/dt)}{[1+k^2\rho_s^2+C|\phi(t)|^2\tau]^2}\\&\quad\times\left(\frac{2[1+(1+\alpha\eta_e)C|\phi(t)|^2\tau]}{[1+k^2\rho_s^2+C|\phi(t)|^2\tau]}-(1+\alpha\eta_e)\right),\end{aligned} \tag{25}$$

where

$$\gamma_m(t)=\frac{(\sqrt{\epsilon}/\nu_{\rm eff})\omega_*^2[\alpha\eta_e+(1+\alpha\eta_e)k^2\rho_s^2][1+(1+\alpha\eta_e)C|\phi(t)|^2\tau]}{[1+k^2\rho_s^2+C|\phi(t)|^2\tau]^2} \tag{26}$$

is the Markovian growth rate. Equation (25) may be greatly simplified by utilizing the fact that $d\xi_k/dt$ can be written in terms of $d\gamma/dt$, making the non-Markovian part of the growth rate proportional to $d\gamma/dt$. Taking the derivative of Eq. (18) and comparing with Eq. (25), the growth rate expression can be rewritten as

$$\gamma(t)=\gamma_m(t)-\tau\frac{d\gamma}{dt}. \tag{27}$$

This expression is similar to Eq. (24), and indicates that the actual growth rate is the Markovian growth rate plus a non-Markovian correction proportional to $d\gamma/dt$. Note that $\gamma$ varies on the time scale of the relaxation oscillation, making the non-Markovian correction small, as long as the relaxation oscillation time scale is long compared to $\tau$. Equation (27) is a differential equation whose solution yields the slowly evolving growth rate. As indicated earlier, slow time scale variation of the growth rate is driven by the difference between the actual growth rate and its Markovian value. As might be expected, solutions of Eq. (27) indicate that the cycle of the actual growth rate lags behind the cycle of the Markovian growth rate by a correlation time.

The solution of Eq. (27) is closely related to the electron particle flux, or correlation of electron density with the radial flow velocity. Using Eq. (4) to express $n_e$ as a function of $\phi$,

$$\Gamma=\frac{c}{B}\left\langle n_e\frac{\partial\phi}{\partial y}\right\rangle$$
$$=-\frac{c}{B\nu_{\rm eff}}\left\langle\left(\frac{\partial\phi}{\partial t}+(1+\alpha\eta_e)V_D\frac{\partial\phi}{\partial y}\right)\frac{\partial\phi}{\partial y}\right\rangle. \tag{28}$$

Fourier transforming and evaluating the lowest-order contribution using Eq. (16), the electron particle flux becomes

$$\Gamma=\sum_k\hat{\gamma}_k(t)\frac{1}{\sqrt{\epsilon}}\frac{c}{B}k_y|\phi_k(t)|^2, \tag{29}$$

where

$$\hat{\gamma}_k(t)=\frac{\gamma(t)}{\omega^{(0)}}=\frac{\omega_*}{\nu_{\rm eff}}\left(\frac{\alpha\eta_e+(1+\alpha\eta_e)k_2\rho_s^2}{1+\xi_k+k^2\rho_s^2}\right). \tag{30}$$

Because the particle flux is proportional to the normalized growth rate $\hat{\gamma}_k(t)$, it depends on $\xi_k$, and is therefore subject to the same time history process that affects the growth rate. Expanding the normalized growth rate about its Markovian value using Eq. (24), and re-expressing $d\xi_k/dt$ in terms of $d\hat{\gamma}_k(t)/dt$, it is found that the normalized growth rate is driven by the difference of Markovian and actual values, just as is the growth rate:

$$\frac{d\hat{\gamma}_k(t)}{dt}=[\hat{\gamma}_m(t)-\hat{\gamma}_k(t)]\tau^{-1}, \tag{31}$$

where

$$\hat{\gamma}_m(t)=\frac{\omega_*}{\nu_{\rm eff}}\left(\frac{\alpha\eta_e+(1+\alpha\eta_e)k_2\rho_s^2}{1+C|\phi_k(t)|^2\tau+k^2\rho_s^2}\right). \tag{32}$$

Equations (29), (31), and (32), which together determine the electron particle flux, express the fact that the particle flux is nonstationary for dissipative trapped electron mode turbulence. Moreover, as shown in the next section, because the normalized growth rate lags behind its Markovian value, the variations of $\hat{\gamma}_m(t)$ and $|\phi_k(t)|^2$ tend to constructively interfere, making the excursions of the particle flux more extreme than those of the energy.

Memory also affects the coherent eddy damping and incoherent emission rates. Expanding the eddy damping rate $\gamma_{nl}(t)$ and the incoherent emission source $S_{\rm in}=2\ {\rm Re}\ L_k^{-1}\Sigma_{k'}(|\chi_{k,k'}^{(E\times B)}|^2+|\chi_{k,k'}^{(\rm pol)}|^2)|\phi_{k'}|^2|\phi_{k-k'}|^2$ about their Markovian values, the long time variation of these rates can also be described by differential equations like Eqs. (27) and (31), i.e., $d\gamma_{nl}/dt=(\gamma_{nl}^{(m)}-\gamma_{nl})\tau^{-1}$, and $dS_{\rm in}/dt=(S_{\rm in}^{(m)}-S_{\rm in})\tau^{-1}$, where $\gamma_{nl}^{(m)}$ and $S_{\rm in}^{(m)}$ are the Markovian eddy damping rate and incoherent emission source. Description of slow time scale nonstationary behavior in the saturation of dissipative trapped electron mode turbulence nominally requires the differential equations for all three nonlinear rates (the amplitude-dependent growth rate, the coherent eddy damping rate, and the incoherent emission source), as well as the spectrum evolution equation. As will be demonstrated in the next section, relaxation oscillation solutions are possible with a reduced description, which assumes a Markovian eddy damping rate and incoherent emission rate, but retains memory effects in the amplitude-dependent growth rate. The makeup of this reduced description indicates that the essential physics required for relaxation oscillations is that of the finite-amplitude growth rate and its memory. Because the growth rate is weaker at large amplitude than it is at small amplitude, it produces a restoring force for amplitude perturbations. The memory in the growth rate then provides the necessary inertia to sustain an oscillation. Physically, when the energy is displaced below its nominal level of saturation, the increased growth rate drives it back toward the saturation level. However, when the energy reaches the saturation level, memory maintains the growth rate above its equilibrium (saturation) value, thus driving the energy above the saturation level.

## V. NONLINEAR OSCILLATOR MODELS

The complexity of the saturation balance relationships [Eqs. (17), (26), and (27)] generally precludes simple steady-state solutions, such as the mixing length. It is nonetheless desirable to extract from these relationships an idea as to how the amplitude-dependent growth rate and memory effects interact, and what types of dynamical behavior result. To this end, solutions of the saturation balance relationships are modeled by reduction to a low-order system of coupled

oscillators. This is not a reduction to a discrete triplet of interacting modes within the spectrum, but rather represents the coupled energies in bands of wave numbers spanning the spectrum. The simplest model divides the spectrum into low and high wave number components and retains memory effects in the amplitude-dependent growth rate. Transfer between the wave number components has incoherent emission and coherent eddy damping elements and is conservative, consistent with Eq. (17). While this reduction is crude, particularly in the grossness of its spectral resolution, it appears to capture the essential workings of the relaxation oscillation, as observed in simulations.

In using low-order nonlinear oscillator models to represent the dynamical behavior of high-order systems, the effects of spectral resolution (or the number of degrees of freedom) is not the only issue affecting their utility. Solutions of low-order nonlinear oscillator models can be sensitive to small variations in the form of the nonlinearities. Reasonable agreement with simulations might thus be as much a matter of fortuitous choice of the form of the oscillator equations as it is an indication that the oscillator model has captured the essential workings of the full saturation balance equations. In the present case the nonlinearities are constrained to represent coherent damping and incoherent emission, thus giving them a specific form. Additionally, they must conserve energy. These constraints largely fix the from of the oscillator model and exclude many other possibilities for coupled spectrum ranges.

There is, however, ambiguity in the form of the correlation time $\tau$ that enters the coupling coefficients and growth rate equation. This time is a function of frequencies, growth rates, and the amplitudes of nonresolved triplets, and therefore does not generally project directly onto a two-component spectrum model. The form used here is appropriate for weak or moderate turbulence, i.e., the transfer rates are proportional to the square of the fluctuation amplitude. In this regime, the correlation time is not a strong function of amplitude, and it can be realistically and unambiguously modeled, even when the spectrum is projected onto a few components. In contrast, in the strong turbulence regime, the projection onto a few components is problematic. This is because the correlation time depends on amplitudes, and the dependence enters as a sum over the spectrum. If spectrum components evolve cyclically, as occurs in the relaxation oscillations, the sum averages over phases. In the few component projection, however, the correlation time has a strong and physically unrealistic dependence on the oscillation phases of individual spectrum components. As shown below, this results in relaxation oscillation behavior in the two component model for strong turbulence, even when there is no amplitude dependence in the growth rate and no memory. In this case, the nonlinear oscillator model does not provide an accurate representation of the dynamics of a many component spectrum, because relaxation oscillations are not observed in simulations when the amplitude dependence of the growth rate is removed by suppressing the frequency shift.

Labeling the low and high $k$ spectral components of energy as $A$ and $B$, respectively, ($A = \int_{k_0}^{k_1} dk|\phi_k|^2$, $B = \int_{k_1}^{k_2} dk|\phi_k|^2$, where $k_0<k_1<k_2$ are the lowest, the mean, and the highest wave numbers of the spectrum), this model is given by

$$\frac{dA}{dt} = \gamma A - \alpha_1 AB + \beta_1 B^2 - \beta_2 A^2, \tag{33}$$

$$\frac{dB}{dt} = -\mu B + \alpha_1 AB - \beta_1 B^2 + \beta_2 A^2, \tag{34}$$

$$\frac{d\gamma}{dt} = \delta\tau^{-1}\left(\frac{\gamma_0(1+B/B_1)}{(1+B/B_0)^2} - \gamma\right), \tag{35}$$

where $\alpha_1$, $\beta_1$, $\beta_2$, $\mu$, $B_0$, $B_1$, and $\delta$ are constants. Equations (33)–(35) represent the dynamically evolving balance of growth rate, coherent eddy damping, and incoherent emission. In the equation for the long-wavelength component of energy, $\alpha_1$ and $\beta_2$ represent coherent eddy damping, while $\beta_1$ represents incoherent emission. The coefficient $\beta_1$ is generally taken to be much smaller than $\alpha_1$, an ordering that typifies transfer in the long-wavelength regime, where energy is carried dominantly to shorter wavelengths from the unstable modes. The constant $\mu$ is the rate of dissipation at short wavelength. The function $\gamma_0(1+B/B_1)(1+B/B_0)^{-2}$ is the Markovian growth rate, with $\gamma_0$ the ratio of the linear growth rate to the effective collision frequency. Comparing Eq. (35) to Eq. (26), it is evident that $B_0$ and $B_1$ are not independent, but $B_0 = B_1(1+\alpha\eta_e)$. The amplitude dependence of the growth rate is weighted to high $k$ spectrum components by its coupling coefficient, making $B$ the only amplitude appearing in the Markovian growth rate.

Consistent with a weak to moderate turbulence regime, the decorrelation rate is taken to be a constant of order the growth rate, $\tau^{-1} \approx \gamma_0$. This rate governs not only the response of the actual growth rate to excursions away from the Markovian growth rate, but moderates the transfer rates in the spectrum component equations. In Eqs. (35) and (36), the decorrelation rate has been absorbed into the coefficients of the spectral transfer rates. The parameter $\delta$ is a multiplier that allows the decorrelation rate to be artificially varied in order to test the role of memory. With $\delta=1$, memory extends over a correlation time consistent with Eqs. (26) and (27). With $\delta \gg 1$ ($\delta=100$ typically), memory is lost in a small fraction of the correlation time, allowing the actual growth rate to respond artificially fast to the Markovian growth rate as amplitude changes occur. This slaves the growth rate to its Markovian value and effectively suppresses memory.

The solution of Eqs. (33)–(35) with $\mu=1.5$, $\alpha_1=4$, $\beta_1=0.1$, $\beta_2=0.01$, $\gamma_0=0.4$, $B_0=0.1$, $B_1=0.025$, and $\delta=1$ is displayed in Figs. 2 and 3. Figure 2 shows a limit cycle with amplitude variations of the energies of the two spectrum components $A$ and $B$ that are $\sim 100\%$ of their RMS value. Examining the evolution of the long-wavelength energy in relation to that of the short-wavelength energy and the growth rate (Fig. 3), it is evident that a dynamic balance between the evolving transfer rates and growth rate governs the energies. When $A$ exceeds a threshold, it transfers energy to $B$, quickly increasing the magnitude of $B$. As $B$ increases, the growth rate plummets, causing $A$ to decrease. This lowers

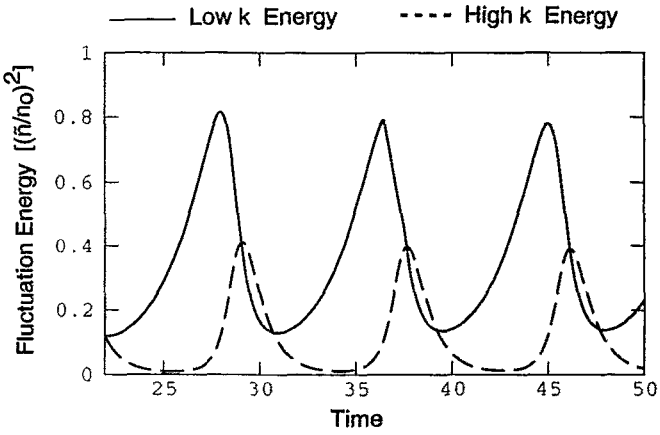


FIG. 2. Temporal evolution of the spectrum energy components for the simple oscillator model, with memory retained in the growth rate.

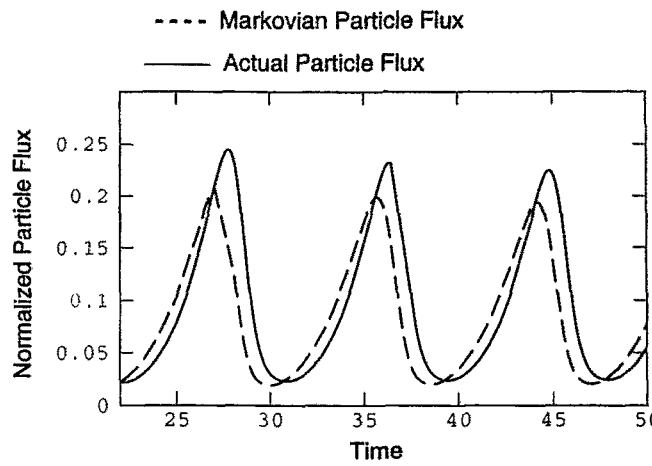


FIG. 4. Temporal evolution of the actual and Markovian particle flux for the dominant spectrum component in the simple oscillator model.

the transfer to $B$, and it decreases under viscous damping. As $B$ decreases, the growth rate increases and returns to its former magnitude. This allows $A$ to increase again to a level where transfer to $B$ is possible, and the cycle restarts. Figure 3 shows the actual growth rate $\gamma$ and the Markovian growth rate $\gamma_M$. The two rates are clearly different, indicating that the usual Markovian assumption is not valid. The actual growth rate lags the Markovian growth rate by a correlation time. Comparing the lag time with the period, it is apparent that the cycle period is about eight times the correlation time in this example. The Markovian growth rate is minimum when the short-wavelength energy is maximum, making the two signals 180° out of phase. Interestingly, the lag experienced by the actual growth rate puts it approximately in phase with the long-wavelength energy. Figure 4 plots the particle flux contribution from long-wavelength modes for the case displayed in Figs. 2 and 3 and compares it with the Markovian flux. A slight time lag is evident; more importantly, the particle flux undergoes a larger fluctuation than the energy because the energy and growth rate components tend to be in phase. This gives the flux a bursty character, a feature also observed in simulations.

The occurrence of limit cycle behavior is not particularly sensitive to changes in the form of the decorrelation rate $\tau^{-1}$ appearing in Eq. (35), provided its magnitude is not strongly affected. For example, using $\gamma$ for $\tau^{-1}$ instead of $\gamma_0$, or even $[\gamma+(A/A_0)^{1/2}]$, where $A_0$ is a constant of order unity, does not change the qualitative behavior of the system. However, changing the magnitude of the decorrelation rate, accomplished here by varying $\delta$, does have a significant effect. To test the role of memory, this parameter was set equal to 100, making the decorrelation rate artificially fast and thereby slaving the growth rate to its Markovian value. As is apparent in Fig. 5, the relaxation oscillations are part of a decaying

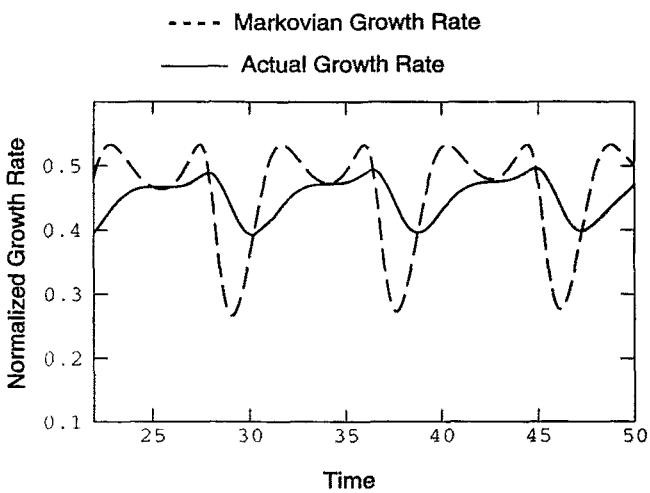


FIG. 3. Temporal evolution of the actual and Markovian growth rates for the simple oscillator model.

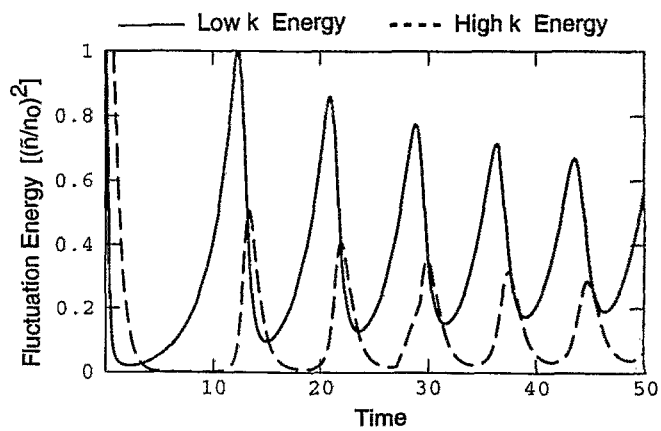


FIG. 5. Time histories of the spectrum energy components for the simple oscillator model. The nonlinear response time of the growth rate to changes in amplitude has been shortened by two orders or magnitude (relative to Fig. 2), effectively slaving the growth rate to the amplitude and thus removing the memory. The relaxation oscillation cannot be sustained and decays to a stable fixed point.

limit cycle that asymptotically approaches a fixed point. The fixed point represents the stationary saturated state usually assumed for dissipative trapped electron mode turbulence. Clearly, memory plays a critical role in the nonstationary character of saturation.

In order to obtain limit cycle behavior, it also appears that the growth rate must decrease for increasing amplitude, i.e., the normalized amplitude $B/B_0$ must be sufficient at its maximum value to access the decaying part of the growth rate curve (see Fig. 1) or sufficient to make the growth rate fall below its value at $B=0$. In the nonlinear oscillator model, this requires $B/B_0>1-2B_1/B_0=1-2/(1+\alpha\eta_e)$ or $B/B_0>B_0/B_1-2=\alpha\eta_e-1$, respectively. For numerical solutions of Eqs. (38)–(40) with $B_0=1$, $B_1=0.25$, and the remaining parameters as in Fig. 2, neither of these conditions is satisfied, and the limit cycle is observed to decay to a fixed point. This supports the interpretation of the relaxation oscillation as being driven by a restoring force associated with a decrease of growth rate when the amplitude is raised above a nominal saturation balance level.

Decomposition of the spectrum into a larger number of components does not affect the basic workings of the relaxation oscillation. With three spectrum components (the low $k$ energy driven by the amplitude-dependent growth rate, the intermediate $k$ energy undriven and undamped, and the high $k$ energy damped by $\mu$) relaxation oscillations like those of Fig. 2 are observed when the growth rate is specified by a memory equation similar to Eq. (35). Likewise, when the growth rate is slaved, the relaxation oscillation decays to a stable fixed point. It is revealing to compare the solutions of the nonlinear oscillator system [Eqs. (33)–(35)] with those of generic three-component nonlinear oscillator models, whose coupling structure is not made to conform to any physical constraints.[8] Whereas limit cycles are common in generic three oscillator models, they appear to occur only under the special circumstances outlined above in models constrained to have nonlinear transfer that is conservative and proportional to a positive power of the energy. This again supports the restoring/inertia picture presented above with the inertia provided by the time history effects of the closure, as opposed to the memory associated with the finite time of transfer in the spectrum. Because exhaustive parameter scans are time consuming, analytical investigation of the stability of fixed points is desirable and will be described elsewhere.

There is an important caveat to the conclusion reached in the previous paragraphs that an amplitude-dependent growth rate and memory are essential elements of the relaxation oscillations. In a two-component spectrum representation that attempts to model the amplitude dependence of the correlation time in a strong turbulence regime, limit cycle solutions are possible, even when the growth rate is fixed and there is no memory. Such a representation is given by

$$\frac{dA}{dt}=\gamma_0 A+\frac{(-\alpha_1 AB+\beta_1 B^2-\beta_2 A^2)}{[\gamma_0+(A/A_0)^{1/2}]}, \tag{36}$$

$$\frac{dB}{dt}=-\mu B+\frac{(\alpha_1 AB-\beta_1 B^2+\beta_2 A^2)}{[\gamma_0+(A/A_0)^{1/2}]}, \tag{37}$$

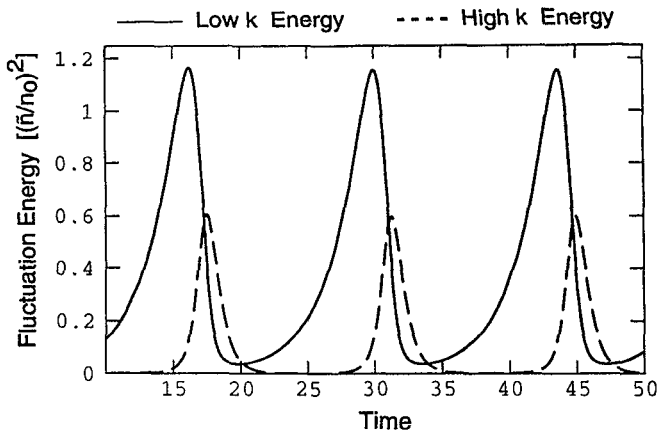


FIG. 6. Time histories of the spectrum energies for a simple oscillator model that incorporates an amplitude-dependent correlation time in the spectral transfer rates. In this model, there is a fixed growth rate and no memory effects. The occurrence of a limit cycle is attributed to a strong (and unphysical) phase coupling between the spectrum energy components and the correlation time.

where the correlation time has been separated from the transfer coefficients and is modeled by a linear correlation time (the growth rate) and a nonlinear time proportional to the square root of the dominant amplitude. Note that for the primary eddy damping term of Eq. (37) (the term proportional to $\alpha_1$), this choice of correlation time yields reasonable weak and strong turbulence limits. Specifically, when $\gamma_0>(A/A_0)^{1/2}$, the transfer rate is proportional to $A$, or amplitude squared, whereas when $\gamma_0<(A/A_0)^{1/2}$, the transfer rate is proportional to $A^{1/2}$, or amplitude to the first power. On the other hand, the $\alpha_1$ term of Eq. (36) has a singular (and unphysical) property in the strong turbulence limit: this term becomes proportional to $A^{1/2}$ and therefore ceases to be a coherent damping rate. This property is linked to the problem discussed earlier in this section, i.e., this correlation time representation has a strong dependence on the phase of the relaxation oscillation. Figure 6 shows the time histories of the long-wavelength and short-wavelength energies for parameter values of $\gamma_0=0.4$, $\alpha_1=4.0$, $\beta_1=0.1$, $\beta_2=0.01$, $\mu=1.5$, and $A_0=1.0$. There is clearly a relaxation oscillation, even though the growth rate is constant, and there is no memory. In simulations of the primitive equations, Eqs. (1)–(3) or Eq. (4), it is possible to access regimes where the frequency shift is small and the growth rate is therefore nearly constant. In these regimes, there is no limit cycle in a strong turbulence limit. As has been discussed, this suggests that in the strong turbulence limit there are difficulties in modeling the correlation time for a two-energy component projection of the spectrum.

## VI. CONCLUSIONS

The frequency shift produced by the cross-coupling of the $E\times B$ and polarization drift nonlinearities in dissipative trapped electron mode turbulence[10,11] has been shown to give rise to a saturated state that is intrinsically nonstationary. In this state, the power density spectrum undergoes a relaxation

oscillation phenomenon driven by the growth rate, as modified by the amplitude-dependent frequency shift. The effective inertia that carries the system past the nominal balance between the amplitude-dependent growth rate and the nonlinear spectral transfer rates has been found to be the memory of the growth rate of prior amplitudes. This memory arises from the time-history integrals over the turbulent response function that occur in statistical closure theory. The memory associated with finite time of transfer in the spectrum (incorporated in the first-order coupled equations for spectrum components) does not support the relaxation oscillation. Rather, it tends to drive the system toward a stationary saturation.

In order to retain memory effects in an energy conserving eddy damping representation, an expansion procedure has been developed that, when applied to the turbulent response function, yields a temporal evolution equation for the amplitude-dependent growth rate. Nonstationary saturation is then described by this equation and the spectrum evolution equation. A simple nonlinear oscillator model based on these equations has been solved in order to demonstrate that the amplitude-dependent growth rate and growth rate memory are necessary for the driving of relaxation oscillations in the saturated state. Solutions of this approximate closure model agree qualitatively with the time-dependent numerical solutions of the original dissipative trapped electron mode turbulence model.[13,14]

This analysis of dissipative trapped electron turbulence has been based on a fluid model that retains the effects of adiabatic electron inertia on the dynamics of nonadiabatic electrons in a single-field description. A two time scale treatment of the model provides an alternate approach to the problem of cross-correlation dynamics, and yields the nonstationary particle flux as the solution of a simple first-order differential equation like that of the growth rate. Under this description, the $E\times B$ nonlinearity is manifestly time dependent, as apparent in the factor $[\omega-\omega_*(1+\alpha\eta_e)]$. This time dependence has been shown to strongly affect the frequency shift induced by the cross-coupling of the $E\times B$ and polarization drift nonlinearities: Because the growth rate is driven by the same factor, frequency shifts that are sufficiently large to force a growing mode to marginal stability, also force the $E\times B$ nonlinearity to zero. However, the $E\times B$ nonlinearity is required for the frequency shift. Thus, the frequency shift that yields marginal stability, i.e., $\omega=\omega_*(1+\alpha\eta_e)$, is the largest shift possible.

The two time scale closure description for nonstationary, non-Markovian saturation was further examined by reducing the spectrum to two components, a long-wavelength energy component driven by the instability and a short-wavelength component damped by viscous dissipation. Energy conservation constraints in the nonlinear coupling were retained in the reduction. The spectrum component evolution equations, together with the equation for the growth rate were found to yield relaxation oscillation solutions driven by the growth rate, with the memory acting as an inertia. The period and amplitude of the oscillations were noted to be similar to those observed in simulations; as was the time history of the *relative* amplitude of the high- and low-energy components. Significantly, when the memory was removed by artificially decreasing the response time of growth rate to changes in the amplitude, the relaxation oscillations become stable and decayed to a fixed point. Similarly, when memory effects were retained in the nonlinear transfer rates, but without the amplitude-dependent growth rate arising from the cross-coupling frequency shift, no sustained relaxation oscillation was observed. While these results are reasonable, they have not been checked over an extensive parameter scan. Analysis of the stability of fixed point solutions to establish analytical criteria for the transition from fixed point to limit cycle behavior is clearly warranted, and will be taken up elsewhere.

This study has underscored the importance of frequency shifts induced at finite amplitude, a phenomenon long overlooked as an important element in the saturation of unstable drift wave fluctuations. Likewise, this study has indicated that memory, also overlooked in simple saturation analyses, is a potentially important effect in transient or nonstationary phenomena at finite amplitude. This includes the relaxation oscillations in the saturated state of dissipative trapped electron mode turbulence, but also potentially includes the intrinsically nonstationary saturation balances involving self-regulated turbulence[22–24] in the L–H mode transition and the dithering H mode. The tools developed herein for the treatment of memory are readily adapted to oscillator models, such as the predator–prey systems used for representing the self-regulated H mode, and will be applied to these problems in future work.

## ACKNOWLEDGMENTS

The authors acknowledge useful discussions with G. G. Craddock, P. H. Diamond, B. A. Carreras, and A. E. Koniges.

This work was supported by U.S. Department of Energy Contract No. DE-FG02-89ER-53291.

[1]L. Garcia, B. A. Carreras, and P. H. Diamond, Phys. Fluids **30**, 1388 (1987).

[2]Throughout this paper, the term growth rate is used as it usually is in turbulence theory, i.e., as referring to both the *e*-folding rate of the amplitude at infinitesimal levels and to the rate of extraction of expansion free energy in saturation (where the amplitude becomes stationary). The latter is quite distinct from the rate of spectral transfer, and is generally assumed to be unaffected by spectral transfer if the eigenmode structure remains invariant in saturation.

[3]P. H. Diamond, P. L. Similon, P. W. Terry, C. W. Horton, S. M. Mahajan, J. D. Meiss, M. N. Rosenbluth, K. Swartz, T. Tajima, R. D. Hazeltine, and D. W. Ross, *Plasma Physics and Controlled Nuclear Fusion Research 1982* (International Atomic Energy Agency, Vienna, 1983), Vol. 1, p. 259; P. W. Terry and P. H. Diamond, in *Statistical Physics and Chaos in Fusion Plasmas*, edited by W. Horton and L. Reichl (Wiley, New York, 1984), p. 335.

[4]P. W. Terry and P. H. Diamond, Phys. Fluids **28**, 1419 (1985).

[5]L. Garcia, P. H. Diamond, B. A. Carreras, and J. D. Callen, Phys. Fluids **28**, 2137 (1985).

[6]B. D. Scott, Phys. Rev. Lett. **65**, 3289 (1990).

[7]B. A. Carreras, K. Sidikman, P. H. Diamond, P. W. Terry, and L. Garcia, Phys. Fluids B **4**, 3115 (1992).

[8]P. W. Terry and W. Horton, Phys. Fluids **26**, 106 (1983).

[9]R. E. Waltz, Phys. Fluids **26**, 169 (1983).

[10]Y.-M. Liang, P. H. Diamond, X. H. Wang, D. E. Newman, and P. W. Terry, Phys. Fluids B **5**, 1128 (1993).

[11]D. E. Newman, P. W. Terry, P. H. Diamond, and Y.-M. Liang, Phys. Fluids B **5**, 1140 (1993).

[12]N. Mattor and P. W. Terry, Phys. Fluids B **4**, 1126 (1992).

[13]D. E. Newman, P. W. Terry, P. H. Diamond, Y.-M. Liang, G. G. Craddock,

A. E. Koniges, and J. A. Crotinger, Phys. Plasmas **1**, 1592 (1994).
[14]P. W. Terry, D. E. Newman, H. Biglari, R. Nazikian, P. H. Diamond, V. B. Lebedev, Y.-M. Liang, V. Shapiro, V. Shevchenko, B. A. Carreras, K. Sidikman, L. Garcia, G. G. Craddock, J. A. Cortinger, and A. E. Koniges, in *Plasma Physics and Controlled Nuclear Fusion Research 1992* (International Atomic Energy Agency, Vienna, 1993), Vol. 2, p. 313.
[15]J. A. Crotinger and T. H. Dupree, Phys. Fluids B **4**, 2854 (1992).
[16]F. Y. Gang, P. H. Diamond, J. A. Crotinger, and A. E. Koniges, Phys. Fluids B **3**, 955 (1991).
[17]A. S. Ware and P. W. Terry, Phys. Plasmas **1**, 658 (1994).
[18]R. H. Kraichnan, J. Fluid Mech. **5**, 497 (1959).
[19]R. M. May, *Stability and Complexity in Model Ecosystems* (Princeton University Press, Princeton, NJ, 1973), pp. 94–108.
[20]G. G. Craddock, A. E. Koniges, P. H. Diamond, D. E. Newman, and P. W. Terry, Phys. Plasmas **1**, 1877 (1994).
[21]S. A. Orszag, J. Fluid Mech. **41**, 363 (1970).
[22]P. H. Diamond, Y.-M. Liang, B. A. Carreras, and P. W. Terry, Phys. Rev. Lett. **72**, 2565 (1994).
[23]B. A. Carreras, D. Newman, P. H. Diamond, and Y.-M. Liang, Phys. Plasmas **1**, 4014 (1994).
[24]P. H. Diamond, Y. M. Liang, and V. B. Lebedev, Bull. Am. Phys. Soc. **38**, 1910 (1993).